Assessment of epidermal growth factor receptor with ^{99m}Tc–ethylenedicysteine–C225 monoclonal antibody

Naomi R. Schechter[a], David J. Yang[b], Ali Azhdarinia[b], Sahar Kohanim[b], Richard WendtIII[b], Chang-Sok Oh[b], Mickey Hu[b], Dong-Fang Yu[b], Jerry Bryant[b], K. Kian Ang[a], Kenneth M. Forster[a], E. Edmund Kim[b] and Donald A. Podoloff[b]

Epidermal growth factor receptor (EGFR) plays an important role in cell division and cancer progression, as well as angiogenesis and metastasis. Since many tumor cells exhibit the EGFR on their surface, functional imaging of EGFR provides not only a non-invasive, reproducible, quantifiable alternative to biopsies, but it also greatly complements pharmacokinetic studies by correlating clinical responses with biological effects. Moreover, molecular endpoints of anti-EGFR therapy could be assessed effectively. C225 is a chimeric monoclonal antibody that targets the human extracellular EGFR and inhibits the growth of EGFR-expressing tumor cells. Also, it has been demonstrated that C225, in combination with chemotherapeutic drugs or radiotherapy, is effective in eradicating well-established tumors in nude mice. We have developed ^{99m}Tc-labeled C225 using ethylenedicysteine (EC) as a chelator. This study aimed at measuring uptake of ^{99m}Tc–EC–C225 in EGFR$^+$ tumor-bearing animal models and preliminary feasibility of imaging patients with head and neck carcinomas. *In vitro* Western blot analysis and cytotoxicity assays were used to examine the integrity of EC–C225. Tissue distribution studies of ^{99m}Tc–EC–C225 were evaluated in tumor-bearing rodents at 0.5–4 h. *In vivo* biodistribution of ^{99m}Tc–EC–C225 in tumor-bearing rodents showed increased tumor-to-tissue ratios as a function of time. *In vitro* and biodistribution studies demonstrated the possibility of using ^{99m}Tc–EC–C225 to assess EGFR expression. SPECT images confirmed that the tumors could be visualized with ^{99m}Tc–EC–C225 from 0.5 to 4 h in tumor bearing rodents. We conclude that ^{99m}Tc–EC–C225 may be useful to assess tumor EGFR expression. This may be useful in the future for selecting patients for treatment with C225. *Anti-Cancer Drugs* 14:49–56 © 2003 Lippincott Williams & Wilkins.

Anti-Cancer Drugs 2003, **14**:49–56

Keywords: antiangiogenesis, epidermal growth factor receptor imaging, ^{99m}Tc–EC–C225

Divisions of [a]Radiation Oncology and [b]Diagnostic Imaging, University of Texas M.D. Anderson Cancer Center, Houston, TX, USA.

Sponsorship: Supported in part by the John S. Dunn Foundation and Cell Point Research Fund (LS01-212). The animal research is supported by M.D. Anderson Cancer Center (CORE) grants NIH CA-16672 and P01 CA-06294.

Correspondence to D.J. Yang, Department of Nuclear Medicine, University of Texas M.D. Anderson Cancer Center, 1515 Holcombe Boulevard, Houston, TX 77030, USA.
Tel: +1 713 794-1053; fax: +1 713-794-5456;
e-mail: dyang@di.mdacc.tmc.edu

Received 16 September 2002 **Accepted** 8 October 2002

Introduction

Traditional cytotoxic approaches to tumor management are beneficial for a number of neoplasms, but are also associated with toxicity. Therefore, more specific molecular targeted interventions have gained attention. An example is therapy directed to counteract epidermal growth factor receptor (EGFR), which is overexpressed in many tumors.

EGFR signaling is not only critical for cell proliferation, but it affects other processes that are crucial to cancer progression, including angiogenesis, metastatic spread and the inhibition of apoptosis. Blockade of the EGFR and its ligands provides a novel approach to cancer treatment [1–3].

C225 is a chimeric monoclonal antibody (mAb) that targets human extracellular EGFR. Several studies have shown that C225 inhibits growth of EGFR-expressing tumor cells *in vitro* and treatment with C225 results in marked inhibition of tumor growth in nude mice bearing xenografts of human cancer cell lines [4,5]. Also, treatment with C225 in combination with chemotherapeutic drugs or radiotherapy is effective in eradicating well-established tumors in nude mice [6–10].

Due to favorable physical characteristics as well as extremely low cost, ^{99m}Tc has been preferred for labeling radiopharmaceuticals. Several compounds have been labeled with ^{99m}Tc using nitrogen and sulfur chelates [11,12]. Bis-aminoethanethiol tetradentate ligands, also called diaminodithiol compounds, are known to form very stable Tc(V)O complexes on the basis of efficient binding of the oxotechnetium group to two thiolsulfur and two amine nitrogen atoms. ^{99m}Tc–L,L-ethylenedicysteine (^{99m}Tc–EC) is a recent and successful example of N_2S_2

0959-4973 © 2003 Lippincott Williams & Wilkins

Copyright © Lippincott Williams & Wilkins. Unauthorized reproduction of this article is prohibited.

chelates. EC can be labeled with ^{99m}Tc easily and efficiently with high radiochemical purity and stability, and is excreted through kidney by active tubular transport [13,14]. A series of ^{99m}Tc–EC–agent conjugates for functional imaging in oncology have been previously reported [15–19]. We have formulated ^{99m}Tc–EC–C225 using EC as a chelator to address a hypothesis that the magnitude of C225 uptake, measured with a radiolabeled C225 scan, may aid in selection of patients for anti-EGFR treatment and prediction of its outcome. In this paper, tumor uptake of ^{99m}Tc–EC–C225 in several EGFR$^+$ cell lines, two different animal models and one patient case is presented. Because overexpression and autocrine activation of EGFR is detected in 90% of head and neck squamous cell carcinoma (HNSCC) [20–22], preliminary imaging feasibility of ^{99m}Tc–EC–C225 was conducted in patients with HNSCC.

Materials and methods

Sulfo-*N*-hydroxysuccinimide (Sulfo-NHS) and 1-ethyl-3-(3-dimethylaminopropyl) carbodiimide–HCl (EDC) were purchased from Pierce (Radford, IL), and Sephadex (G-25) was purchased from Sigma (St Louis, MO). All other chemicals were purchased from Aldrich (Milwaukee, WI). ^{99m}Tc-pertechnetate was obtained from a commercial ^{99}Mo/^{99m}Tc generator (Ultratechnekow FM; Mallinckrodt Diagnostica, Houston, TX).

Radiosynthesis of ^{99m}Tc–EC–C225

Synthesis of EC was prepared in a two-step manner according to the previously described methods [23,24]. The precursor, L-thiazolidine-4-carboxylic acid, was synthesized (m.p. 195°C, reported 196–197°C). EC was then prepared (m.p. 247°C, reported 251–253°C). The structure was confirmed by ^{1}H-NMR and mass spectroscopy (FAB-MS) m/z 268 (M^+, 100).

Clinical grade anti-EGFR mAb C225 (IMC-C225) was obtained from the ImClone Systems (Somerville, NJ). C225 (20 mg) was stirred with EC (28.8 mg, 0.11 mmol in 1.4 ml of 1 N $NaHCO_3$), Sulfo-NHS (23.3 mg, 0.11 mmol) and EDC (16.6 mg, 0.09 mmol). After dialysis, 17 mg of EC–C225 was obtained. Then 100 mCi of $Na^{99m}TcO_4$ was added into a vial containing 1 mg EC–C225 and 100 μg $SnCl_2$, and the product was purified with a G-25 column and eluted with PBS, yielding 80 mCi ^{99m}Tc–EC–C225.

Integrity of EC–C225

An immunoassay (Western blot and immunoprecipitation) and cell proliferation assays were used to examine the integrity of EC–C225. Western Blot analysis was also performed on A431 (EGFR expression cell line, positive control), MDA231 (medium EGFR expression) and MDA453 (poor EGFR expression, negative control). Cells were treated with C225 or EC–C225 (10 μg) and then lysed with buffer containing 20% SDS in dimethyl formamide/H_2O, pH 4.7, at 37°C. The supernatants were cleared by centrifugation and the protein concentrations were measured by the Lowry method. Equal amounts of protein were subjected to immunoprecipitation in the presence of mouse antihuman EGFR antibody (Oncogene, Boston, MA) for 2 h at 4°C, followed by incubation with immobilized Protein G plus/Protein A–agarose beads (Oncogene) overnight at 4°C. For Western immunoblotting, the immunoprecipitates or equal amounts of crude extract were boiled in Laemmli SDS sample buffer, resolved by SDS–PAGE, transferred to nitrocellulose and probed with mouse antiphosphorylation primary antibody (Upstate Biotechnology, Lake Placid, NY) at 4°C overnight. After the blots were incubated for another 1 h at room temperature with horseradish peroxidase-labeled anti-mouse secondary antibody (Amersham Life Science, Arlington Heights, IL), signals were detected by the enhanced chemiluminescence assay (Amersham Life Science) according to the manufacturer's instructions.

DiFi cells are known to undergo apoptosis when exposed to C225 in culture. For cell viability assays, cells were seeded onto 24-well culture plates and exposed to the appropriate amounts of C225, EC–C225 or EC sodium salt alone (control) for 24 h incubation. Subsequently, 50 μl of 10 mg/ml MTT (Sigma) was added into 0.5 ml of culture medium and the cells incubated for 3 h at 37°C in a CO_2 incubator, followed by cell lysis with buffer containing 20% SDS in dimethyl formamide/H_2O, pH 4.7, at 37°C for more than 6 h. Cell viability was then determined by measuring the optical absorbance of cell lysate at a wavelength of 595 nm and normalizing the value with the corresponding untreated cells.

In vitro cellular uptake assay

To evaluate if the uptake of ^{99m}Tc–EC–C225 correlates to EGFR density, *in vitro* cellular uptake assay was conducted using high and intermediate EGFR-expressing human cancer cell lines A431 and MDA 231, respectively. Each well containing 80 000 cells was exposed to 2 μCi ^{99m}Tc–EC–C225. After 2-h incubation, the cells were washed with phosphate-buffered saline 3 times and followed by trypsinization. The cells were counted by a γ-counter.

Tissue distribution studies

The animal experiments were approved by the University of Texas M. D. Anderson Institutional Animal Care and Use Committee (IACUC). Biodistribution was assessed in A431 grown in nude mice (1 μCi/mouse, 10 μg/mouse, $n = 3$/time interval, i.v.) or 13762 NF grown in rats (15–20 μCi/rat, i.v.). Female rodents were inoculated s.c. with 0.1 ml of tumor cells suspension, containing 10^6 cells into the hind legs using 25-gauge needles. Studies were performed 14–17 days after implantation when tumors

Copyright © Lippincott Williams & Wilkins. Unauthorized reproduction of this article is prohibited.

reached approximately 1 cm diameter. Following administration of the radiotracer, 10 μg ^{99m}Tc–EC–C225 per animal, the rodents were sacrificed at 0.5 and 4 h. The selected tissues were excised, weighed and counted for radioactivity by using a γ-counter (Packard Instruments, Downers Grove, IL). The biodistribution of tracer in each sample was calculated as percentage of the injected dose per gram of tissue wet weight (%ID/g). Tumor:non-target tissue count density ratios were calculated from the corresponding %ID/g values. Student's *t*-test was used to assess the significance of differences between groups. The same procedure was followed for *in vivo* blocking studies by administering cold C225 to the blocking group 30 min prior to the injection of the radiotracer.

Scintigraphic imaging study

^{99m}Tc–EC–C225 (22 mCi; 0.05 mg) was administered i.v. to a patient with locally advanced squamous cell carcinomas of the head and neck. To ascertain the optimal time for tumor visualization, SPECT scans including the region of interest (ROI) were obtained at 2, 4 and 6 h after injection. The SPECT imaging was obtained by a γ-camera (Siemens Medical Systems, Hoffman Estates, IL) equipped with low-energy, parallel-hole collimator, using 45 stops in approximately 25 min (30 s/stop), and images were reconstructed using a Hamming filter in 128 × 128 matrix format. SPECT scan findings were compared to CT scan findings.

Results

Radiosynthesis of ^{99m}Tc–EC–C225

Radiochemical purity for ^{99m}Tc–EC–C225 was 100% (HPLC, gel permeation column, 0.1%. LiBr in 10 mM PBS, pH 7.4). Specific activity was 2 Ci/μmol (Fig. 1).

Fig. 1

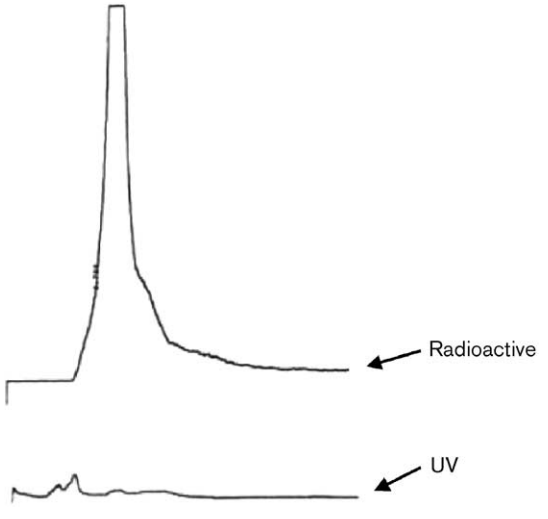

HPLC analysis of ^{99m}Tc–EC–C225 indicated that radiochemical purity was 100%. The specific activity of ^{99m}Tc–EC–C225 was 2 Ci/μmol.

Integrity of EC–C225

No significant differences were found between labeled and unlabeled C225 in affinity. Western immunoblotting and immunoprecipitation showed different intensities among, A431 (EGFR expression cell line, positive control), MDA231 (medium EGFR expression) and MDA453 (poor EGFR expression, negative control), the three cell lines (Fig. 2A). The result showed that EC–C225 is biologically active in inducing cell death in DiFi cells. In contrast, the EC-Na did not show any effect on cell proliferation when compared with control. There was no significant difference found between labeled and unlabeled C225 in inhibiting cell growth (Fig. 2B).

In vitro cellular uptake assay

There was a marked cellular uptake difference between A431 and MDA 231 cell lines. A431, a known EGFR expression cell line, showed higher uptake than MDA231 (Fig. 3).

Tissue distribution studies

Biodistribution studies showed that tumor-to-muscle count density ratios increased as a function of time in A431 tumor-bearing mice and breast tumor-bearing rats (Figs 4 and 5). Tumor-to-muscle count density ratios reached a plateau at 2 and 4 h, respectively. At 2 h tumor uptake (%ID/g) was 0.309% for ^{99m}Tc–EC–C225 (Table 1) and 0.115% for ^{99m}Tc–EC (control) (Table 2). At 4 h tumor uptake (%ID/g) was 0.26% for ^{99m}Tc–EC–C225 (Table 1) and 0.096% for ^{99m}Tc–EC (control) (Table 2). Receptor blocking studies showed decreased tumor-to-muscle count density ratios at 2 h post-administration of ^{99m}Tc–EC–C225 (Fig. 6).

Scintigraphic imaging study

A selected image of one patient imaged with ^{99m}Tc–EC–C225 is illustrated in Fig. 7. The patient had squamous cell carcinoma of the left tonsil (arrow) metastatic to left neck lymph nodes. The patient had already undergone planning for radiation therapy treatment. The patient wore a radiation therapy plastic immobilization mask during the ^{99m}Tc–EC–C225 SPECT imaging scans. Enhancement of three fiducial markers was seen at 12:00, 3:00 and 9:00. The SPECT images were then fixed with axial slices of the radiation therapy planning computed tomography. The ^{99m}Tc–EC–C225 SPECT images showed that the primary tumor but not the nodal sites could be well visualized at 2 h post-administration.

Discussion

Studies have suggested neovascularization as a requirement for primary tumor growth, invasion and metastasis. Reports also give evidence that acquisition of the angiogenic phenotype is a common pathway for tumor progression and that active angiogenesis is associated with other molecular mechanisms leading to tumor

Copyright © Lippincott Williams & Wilkins. Unauthorized reproduction of this article is prohibited.

Fig. 2

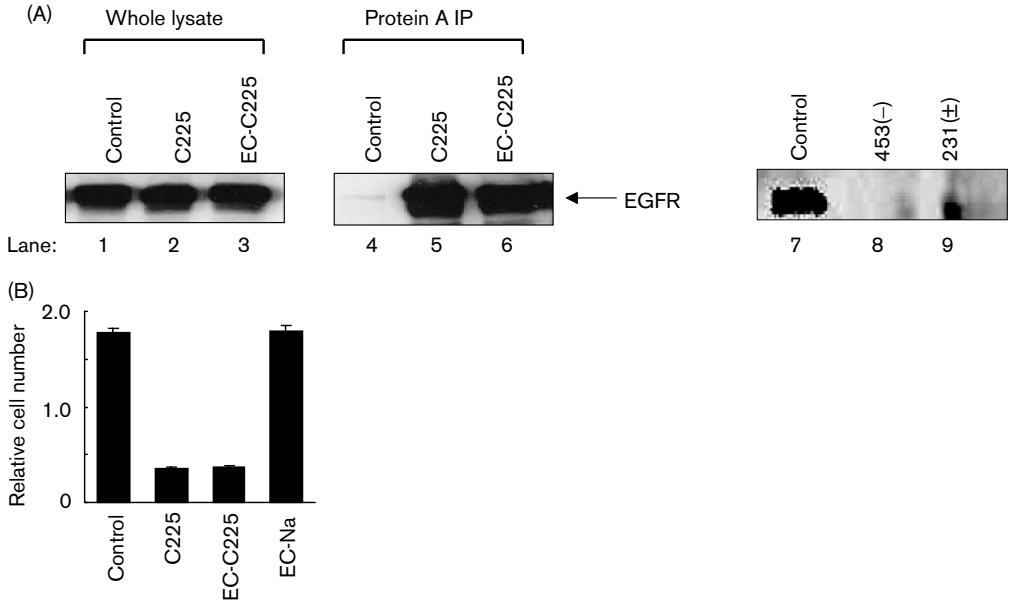

Western immunoblotting and immunoprecipitation (A) and cell viability assays (B) showed no changes in the integrity of EC–C225 compared to C225.

Fig. 3

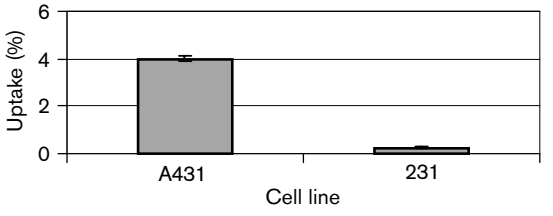

In vitro cellular uptake assays of ^{99m}Tc–EC–C225 in two cell lines. A431, a standard EGFR expression cell line, showed higher uptake than MDA 231.

progression [25–28]. There are four types of antiangiogenic therapy agents [29–32]. They are (i) antibodies, such as anti-integrins (Vitaxin), anti-EGFR (C225), anti-VEGF mAb, anti-endoglin glycoprotein (anti-TGF-β); (iii) protein fragments, such as plasminogen and collagen (angiostatin, endostatin, vasostatin, canstatin, restin, thromospondin); (iii) modulation of fibroblast growth factors (interferons); and (iv) synthetic small molecules, such as protease inhibitors (marimastat, prinomastat, tanomastat, solimastat, TNP470), urokinase inhibitors, cyclooxygenase inhibitors and tyrosine kinase inhibitors [SU5416, ZD4190 (anti-VEGFR); SU6668 (anti-VEGFR/FGFR/PDGFR); SU5402, SU4984 (anti-FGFR); STI571 (anti-PDGFR); PD173074 (anti-FGFR/VEGFR), ZD1839 and OSI-774 (anti-EGFR)]. These new anti-angiogenic agents represent some of the more promising new approaches to anticancer therapy.

C225, an anti-EGFR antibody, has shown antitumor activity in tumor cells lines expressing EGFR, including heightened radiation response *in vitro* in cultured human squamous cell carcinoma and enhancement of taxane- and platinum-induced cytotoxicity in non-small cell lung cancer xenografts [22]. In A431 head and neck squamous cell xenografts, C225 administered both before and after radiation therapy yields a radiation enhancement factor of 3.62, attributable to both tumor necrosis and antiangiogenesis [7,10]. The preclinical and clinical efficacy of C225 appears to involve multiple anticancer mechanisms; however, there are no molecular markers to assess C225 endpoint. The ability to assess tumor EGFR expression and C225 uptake by ^{99m}Tc-labeled C225 would allow selection of proper patient population to evaluate the efficiency of anti-EGFR therapy for cancer.

Imaging with ^{99m}Tc–EC–C225 has the following potential advantages over biopsy: (i) non-invasive, (ii) reproducible, (iii) easily quantifiable, (iv) can be used to access areas which are dangerous to biopsy and (v) can be used to assess the whole body at once. Due to better imaging characteristics and lower price, attempts have been made to replace the ^{123}I-, ^{131}I-, ^{67}Ga- and ^{111}In-labeled compounds with corresponding ^{99m}Tc-labeled compounds when possible. Verbruggen *et al.* [12] reported that EC can be labeled with ^{99m}Tc easily and efficiently at room temperature with high radiochemical purity, and the preparation remains stable for at least 8 h. Recently, our laboratory developed a series of EC–drug conjugates

Copyright © Lippincott Williams & Wilkins. Unauthorized reproduction of this article is prohibited.

Fig. 4

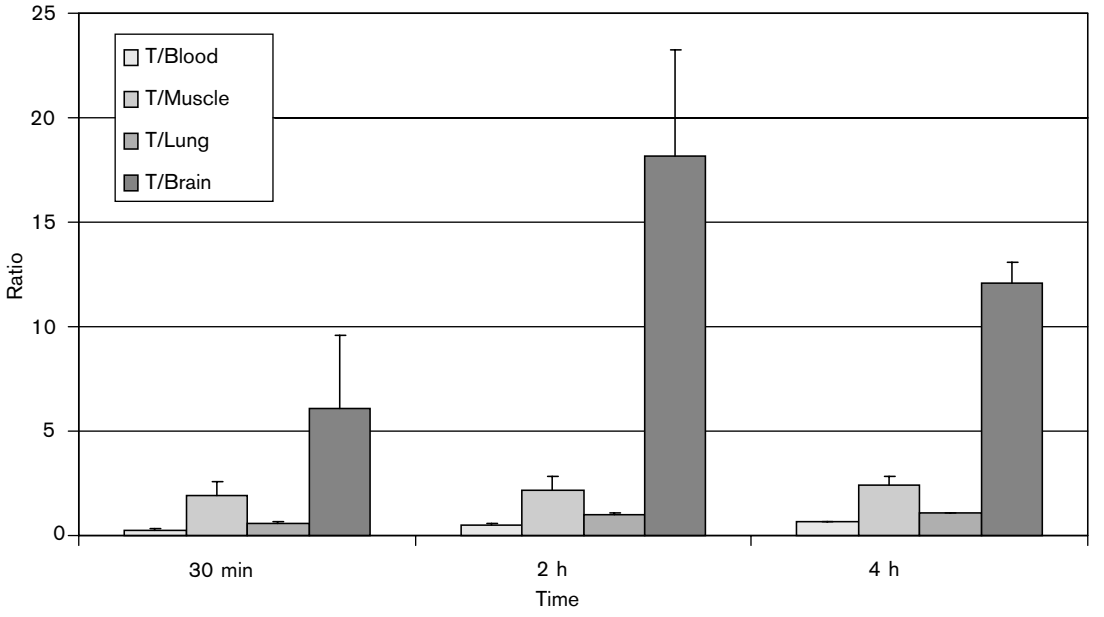

Tumor-to-tissue count density ratios of ^{99m}Tc–EC–C225 in A431 tumor-bearing mice showed an increase as a function of time. Data are expressed as the mean + SE for $n = 3$ rats per group.

Fig. 5

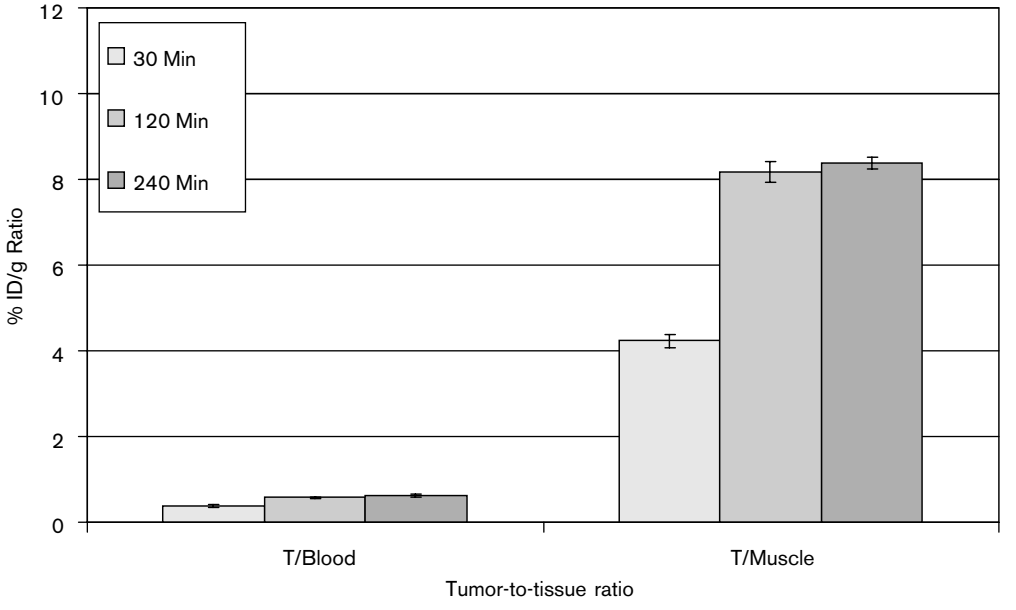

Tumor-to-tissue count density ratios of ^{99m}Tc–EC–C225 in breast tumor-bearing rats showed an increase as a function of time. Data are expressed as the mean + SE for $n = 3$ rats per group.

labeled with ^{99m}Tc [15–19]. In this paper, EC–C225 was prepared using relatively simple and rapid synthesis.

In tissue distribution studies, there was a difference in tumor-to-muscle uptake ratio between the ^{99m}Tc–EC–C225 (8 at 2 and 4 h) (Table 1) and ^{99m}Tc–EC (4 at 2 h and 5 at 4 h) (Table 2) groups observed. In addition, the tumor uptake (%ID/g) at 2 and 4 h was greater in the ^{99m}Tc–EC–C225 group (0.309 compared with 0.115 at 2 h and 0.260 compared with 0.096 at 4 h) (Tables 1 and 2).

Copyright © Lippincott Williams & Wilkins. Unauthorized reproduction of this article is prohibited.

Table 1 **Biodistribution of ^{99m}Tc–EC–C225 in breast tumor-bearing rats**

	Percent of injected ^{99}mTc–EC–C225 dose per gram of tissue		
	30 min	2 h	4 h
Blood	1.119±0.132	0.539±0.037	0.414±0.008
Heart	0.284±0.024	0.137±0.011	0.103±0.005
Lung	0.639±0.050	0.315±0.016	0.232±0.024
Liver	0.929±0.146	0.721±0.016	0.582±0.063
Spleen	0.671±0.019	0.428±0.038	0.420±0.050
Kidney	13.832±0.027	14.794± 0.472	12.952±0.522
Intestine	0.280±0.031	0.690±0.400	0.179±0.012
Muscle	0.099±0.003	0.038±0.001	0.031±0.001
Tumor	0.416±0.001	0.309±0.013	0.260±0.016
Thyroid	0.471±0.086	0.229±0.005	0.153±0.015
Stomach	0.418±0.081	0.180±0.029	0.166±0.036

Values shown represent the mean±SD of data from three animals.

Table 2 **Biodistribution of ^{99m}Tc–EC in breast tumor-bearing rats**

	Percent of injected ^{99}mTc–EC dose per gram of tissue			
	30 min	1 h	2 h	4 h
Blood	0.435±0.029	0.273±0.039	0.211±0.001	0.149±0.008
Lung	0.272±0.019	0.187±0.029	0.144±0.002	0.120±0.012
Liver	0.508±0.062	0.367±0.006	0.286±0.073	0.234±0.016
Kidney	7.914±0.896	8.991±0.268	9.116±0.053	7.834±1.018
Intestine	0.173±0.029	0.787±0.106	0.401±0.093	0.103±0.009
Muscle	0.060±0.006	0.043±0.002	0.028±0.009	0.019±0.001
Tumor	0.342±0.163	0.149±0.020	0.115±0.002	0.096±0.005
Thyroid	0.219±0.036	0.229±0.118	0.106±0.003	0.083±0.005
Urine	9.124±0.808	11.045±6.158	13.192±4.505	8.693±2.981
Stomach	0.136±0.060	0.127±0.106	0.037±0.027	0.043±0.014

Values shown represent the mean±SD of data from three animals.

Fig. 6

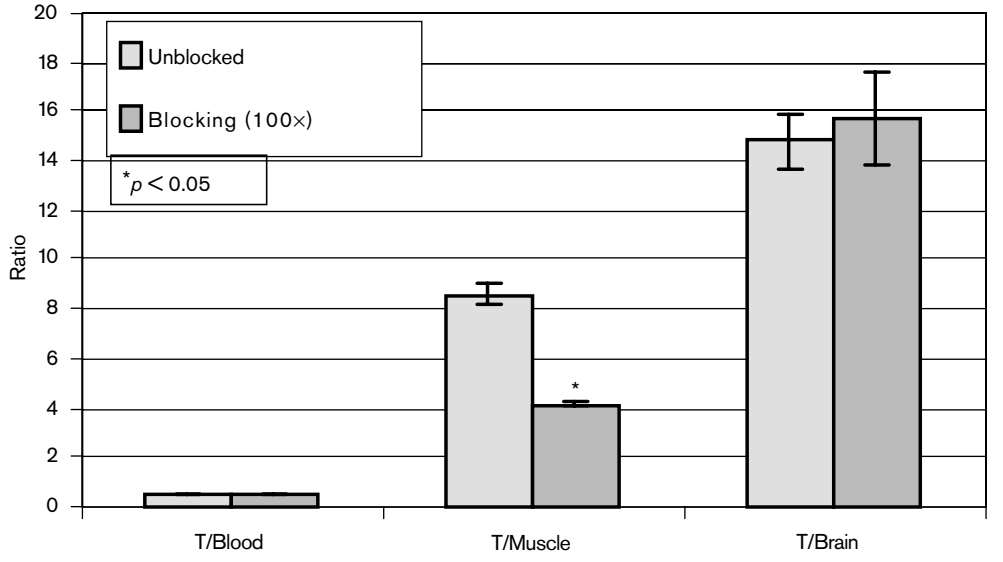

Tumor-to-tissue count density ratios of ^{99m}Tc–EC–C225 in breast tumor-bearing after pre-treatment with C225 showed that tumor-to-muscle count density ratio was decreased at 2 h post-injection.

In comparing the two groups, the washout rate must be taken into consideration when observing the percent uptake in the tissues. Pre-treatment of rats with unlabeled C225 led to a decrease in the tumor-to-muscle count density ratios. The findings suggest that tumor uptake of ^{99m}Tc–EC–C225 occurs via a receptor-

Copyright © Lippincott Williams & Wilkins. Unauthorized reproduction of this article is prohibited.

Fig. 7

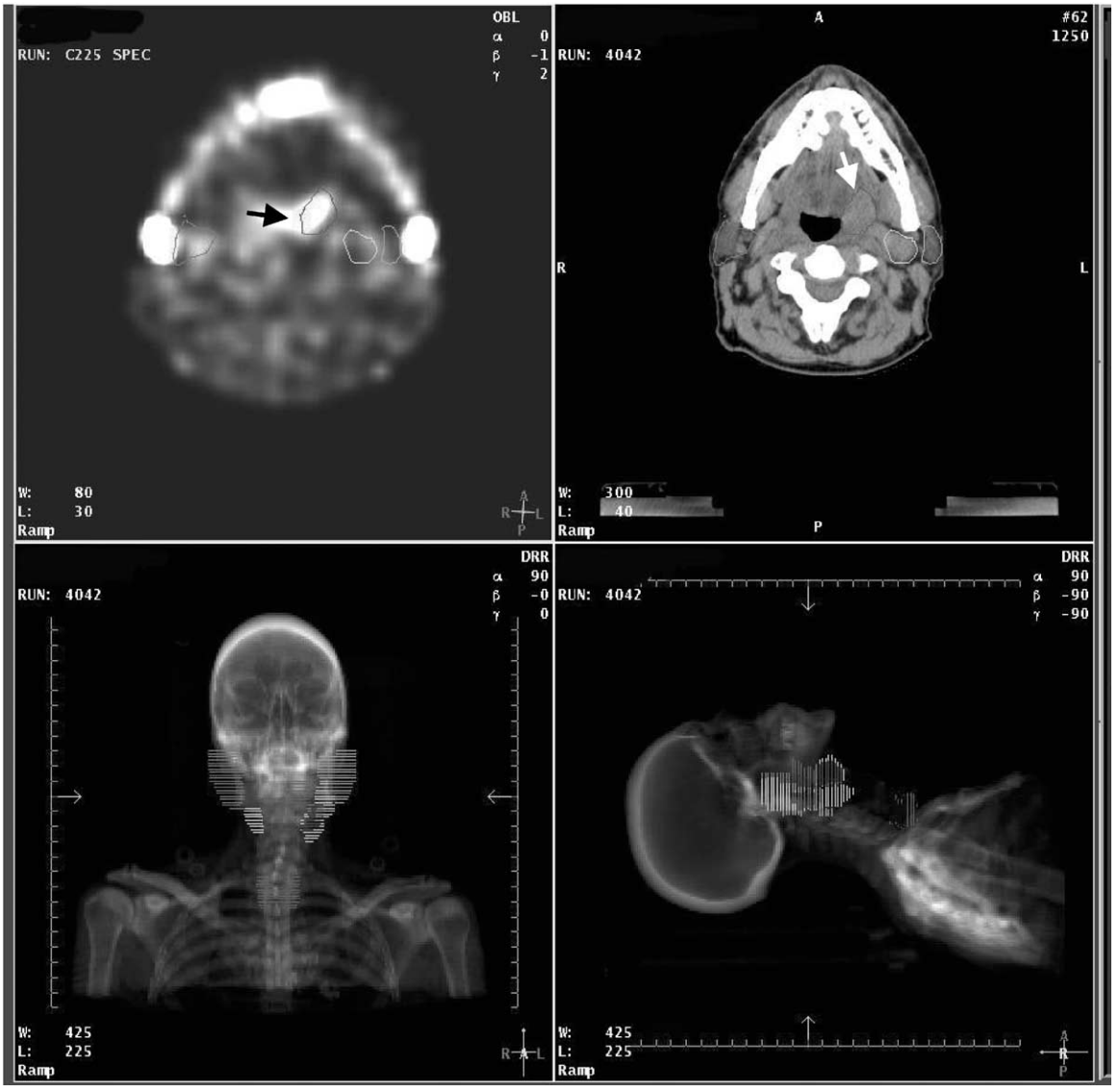

Transaxial view of a patient receiving ^{99m}Tc–EC–C225 (25 mCi, i.v.). The patient had a tumor at the left base of the tongue and the floor of the mouth. Using an imaging overlay technique, ^{99m}Tc–EC–C225 SPECT images showed that the tumor could be visualized at 2 h post-administration using the original color images.

mediated process. Planar imaging of ^{99m}Tc–EC–C225 demonstrated the feasibility to image tumors at 2 h post-injection.

In summary, a convenient and simple method for radiolabeling C225 with high specific activity was achieved. *In vitro* and *in vivo* biodistribution studies demonstrated the feasibility of using ^{99m}Tc–EC–C225 to assess EGFR expression. EGFR is overexpressed in a significant percentage of human A431 cells which correlates well with ^{99m}Tc–EC–C225 uptake. Our animal studies and preliminary clinical imaging studies suggest that ^{99m}Tc–EC–C225, a specific marker for EGFR, may be useful in selecting patients most likely to benefit from C225 therapy.

Acknowledgments

The authors wish to thank Eloise Daigle for her secretarial support.

References

1 Waxman ES, Herbst RS. The role of the epidermal growth factor receptor in the treatment of colorectal carcinoma. *Semin Oncol Nurs* 2002; **18**:20–29.

2 Jung YD, Mansfield PF, Akagi M, Takeda A, Liu W, Bucana CD, *et al.* Effects of combination anti-vascular endothelial growth factor receptor and anti-epidermal growth factor receptor therapies on the growth of gastric cancer in a nude mouse model. *Eur J Cancer* 2002; **38**:1133–1140.

Copyright © Lippincott Williams & Wilkins. Unauthorized reproduction of this article is prohibited.

3 Ciardiello F, Tortora G. A novel approach in the treatment of cancer: targeting the epidermal growth factor receptor. *Clin Cancer Res* 2001; **7**:2958–2970.

4 Karashima T, Sweeney P, Slaton JW, Kim SJ, Kedar D, Izawa JI, *et al.* Inhibition of angiogenesis by the antiepidermal growth factor receptor antibody ImClone C225 in androgen-independent prostate cancer growing orthotopically in nude mice. *Clin Cancer Res* 2002; **8**:1253–1264.

5 Kim ES, Khuri FR, Herbst RS. Epidermal growth factor receptor biology (IMC-C225). *Curr Opin Oncol* 2001; **13**:506–513.

6 Prewett MC, Hooper AT, Bassi R, Ellis LM, Waksal HW, Hicklin DJ. Enhanced antitumor activity of anti-epidermal growth factor receptor monoclonal antibody IMC-C225 in combination with irinotecan (CPT-11) against human colorectal tumor xenografts. *Clin Cancer Res* 2002; **8**:994–1003.

7 Herbst RS, Langer CJ. Epidermal growth factor receptors as a target for cancer treatment: the emerging role of IMC-C225 in the treatment of lung and head and neck cancers. *Semin Oncol* 2002; **29**:27–36.

8 Burke PA, DeNardo SJ, Miers LA, Kukis DL, DeNardo GL. Combined modality radioimmunotherapy. Promise and peril. *Cancer* 2002; **94**:1320–1331.

9 Harari PM, Huang SM. Radiation response modification following molecular inhibition of epidermal growth factor receptor signaling. *Semin Radiat Oncol* 2001; **11**:281–289.

10 Nasu S, Ang KK, Fan Z, Milas L. C225 antiepidermal growth factor receptor antibody enhances tumor radiocurability. *Int J Radiat Oncol Biol Phys* 2001; **51**:474–477.

11 Davison A, Jones AG, Orvig C, Sohn M. A new class of oxotechnetium(+5) chelate complexes containing a $TcON_2S_2$ core. *Inorg Chem* 1981; **20**:1629–1632.

12 Verbruggen AM, Nosco DL, Van Nerom CG, Bormans GM, Adriaens PJ, De Roo MJ. Tc-99m–L,L-ethylenedicysteine: a renal imaging agent. I. Labelling and evaluation in animals. *J Nucl Med* 1992; **33**:551–557.

13 Van Nerom CG, Bormans GM, De Roo MJ, Verbruggen AM. First experience in healthy volunteers with Tc-99m–L,L-ethylenedicysteine, a new renal imaging agent. *Eur J Nucl Med* 1993; **20**:738–746.

14 Surma MJ, Wiewiora J, Liniecki J. Usefulness of Tc-99m–*N,N′*-ethylene-1-dicysteine complex for dynamic kidney investigations. *Nucl Med Commun* 1994; **15**:628–635.

15 Ilgan S, Yang DJ, Higuchi T, Zareneyrizi F, Bayhan H, Yu DF, *et al.* ^{99m}Tc–Ethylenedicysteine–folate: a new tumor imaging agent. Synthesis, labeling and evaluation in animals. *Cancer Biother Radiopharm* 1998; **13**:427–435.

16 Zareneyrizi F, Yang DJ, Oh C-S, Ilgan S, Yu DF, Tansey W, *et al.* Synthesis of ^{99m}Tc–ethylenedicysteine–colchicine for evaluation of antiangiogenic effects. *Anti-Cancer Drugs* 1999; **10**:685–692.

17 Yang DJ, Ilgan S, Higuchi T, Zareneyrizi F, Oh C-S, Liu C-W, *et al.* Noninvasive assessment of tumor hypoxia with ^{99m}Tc-labeled metronidazole. *Pharm Res* 1999; **16**:743–750.

18 Yang DJ, Azhdarinia A, Wu P, Yu DF, Tansey W, Kohanim S, *et al. In vivo* and *in vitro* measurement of apoptosis in breast cancer cells using ^{99m}Tc–EC–Annexin V. *Cancer Biother Radiopharm* 2001; **16**:73–84.

19 Yang DJ, Kim K-D, Schechter NR, Yu DF, Wu P, Azhdarinia A, *et al.* Assessment of antiangiogenic effect using ^{99m}Tc–EC–endostatin. *Cancer Biother Radiopharm* 2002; **17**:233–246.

20 Bonner JA, De Los Santos J, Waksal HW, Needle MN, Trummel HQ, Raisch KP. Epidermal growth factor receptor as a therapeutic target in head and neck cancer. *Semin Radiat Oncol* 2002; **12**:11–20.

21 Bancroft CC, Chen Z, Yeh J, Sunwoo JB, Yeh NT, Jackson S, *et al.* Effects of pharmacologic antagonists of epidermal growth factor receptor, PI3 K and MEK signal kinases on NF-kappaB and AP-1 activation and IL-8 and VEGF expression in human head and neck squamous cell carcinoma lines. *Int J Cancer* 2002; **99**:538–548.

22 Herbst RS, Kim ES, Harari PM. IMC-C225, an anti-epidermal growth factor receptor monoclonal antibody, for treatment of head and neck cancer. *Expert Opin Biol Ther* 2001; **1**:719–732.

23 Ratner S, Clarke HT. The action of formaldehyde upon cysteine. *J Am Chem Soc* 1937; **59**:200–206.

24 Blondeau P, Berse C, Gravel D. Dimerization of an intermediate during the sodium in liquid ammonia reduction of L-thiazolidine-4-carboxylic acid. *Can J Chem* 1967; **45**:49–52.

25 Sion-Vardy N, Fliss DM, Prinsloo I, Shoham-Vardi I, Benharroch D. Neoangiogenesis in squamous cell carcinoma of the larynx—biological and prognostic associations. *Pathol Res Pract* 2001; **197**:1–5.

26 Guang-Wu H, Sunagawa M, Jie-En L, Shimada S, Gang Z, Tokeshi Y, *et al.* The relationship between microvessel density, the expression of vascular endothelial growth factor (VEGF), and the extension of nasopharyngeal carcinoma. *Laryngoscope* 2000; **110**:2066–2069.

27 Xiangming C, Hokita S, Natsugoe S, Tanabe G, Baba M, Takao S, *et al.* Angiogenesis as an unfavorable factor related to lymph node metastasis in early gastric cancer. *Ann Surg Oncol* 1998; **5**:585–589.

28 Ugurel S, Rappl G, Tilgen W, Reinhold U. Increased serum concentration of angiogenic factors in malignant melanoma patients correlates with tumor progression and survival. *J Clin Oncol* 2001; **19**:577–583.

29 Feltis BA, Sahar DA, Kim AS, Saltzman DA, Leonard AS, Sielaff TD. Cyclooxygenase-2 inhibition augments the hepatic antitumor effect of oral *Salmonella typhimurium* in a model of mouse metastatic colon cancer. *Dis Colon Rectum* 2002; **45**:1023–1028.

30 Decatris M, Santhanam S, O'Byrne K. Potential of interferon-alpha in solid tumours: part 1. *BioDrugs* 2002; **16**:261–281.

31 Baselga J, Albanell J. Targeting epidermal growth factor receptor in lung cancer. *Curr Oncol Rep* 2002; **4**:317–324.

32 Herbst RS, Shin DM. Monoclonal antibodies to target epidermal growth factor receptor-positive tumors: a new paradigm for cancer therapy. *Cancer* 2002; **94**:1593–1611.

Copyright © Lippincott Williams & Wilkins. Unauthorized reproduction of this article is prohibited.